

The influence of aging on buckle strength loss in AA5182-H48 for beverage can ends

Paweł Kokoszka^{1*} , Andrij Milenin² 

¹CANPACK S.A., Business Support Service, Starowiejska 28 Street, 32-800 Brzesko, Poland.

²AGH University of Krakow, Faculty of Metals Engineering and Industrial Computer Science, al. A. Mickiewicza 30, 30-059 Krakow, Poland.

Abstract

The paper examines the influence of aging on buckling strength loss for aluminum alloy 5182 beverage can ends. In the experimental study, aging took place naturally and artificially. For the buckling strength testing, a special experimental technique was used, which was based on measuring the internal pressure leading to the destruction of the beverage can ends. The experimental results show that the beverage can ends indicate a significant time-dependent buckle strength loss. For example, a year of aging can end at 20°C leading to a decrease in its strength by 5%. Half of this decrease occurs in the first 3–4 weeks. The aging phenomenon also got worse with increasing temperature. It has been found that increasing the aging temperature to 40°C results in an 8% reduction in buckling strength after 4 weeks of aging. The whole life cycle, from its production to the processes it undergoes and storage time, was analyzed. At the same time, tests were carried out for both the input material and the product itself. On this basis, the mechanical properties and their change depending on time or temperature were examined. All specimens made from can end stock (CES) were also found to not show the same drop of mechanical properties as for the buckling of finished ends. The obtained experimental allowed the development of an empirical mathematical model that makes it possible to predict the buckling strength of the can end depending on the conditions of aging and temperature of testing. The present study showed the importance of temperature conditions used in can filling lines in the determination of resistance to changes in buckling for the ends.

Keywords: AA5182-H48 alloy, beverage end, aging, buckling strength, manufacturing process

1. Introduction

Aluminum alloys are used for a wide range of applications in various industries (Cayless, 1990; Hosford & Duncan, 1994; McMahon et al., 2017). The unique combinations of properties provided one of the most versatile applications, from the automotive industry (Gong et al., 2019) through the aerospace industry to beverage packaging (Kaufman, 2000).

In the last few years, the can-making industry has become a very fast-growing one. The main product of

this industry is two-piece aluminium cans, consisting of cans and ends (Hosford & Duncan, 1994). These two products have long been made of aluminium alloys (Hoyle & Setlak, 1996; Yang et al., 2020; Zhu & Starink, 2008).

It is known that the mechanical properties of these alloys affect the technology of forming during production (Wędrychowicz et al., 2021). In the work by Baran et al. (2022), it is experimentally shown that the destruction of the material of the can during the production process is associated with the chemical

*Corresponding author: pawel.kokoszka@canpack.com

ORCID ID's: 0000-0003-3864-7873 (P. Kokoszka), 0000-0002-6266-2881 (A. Milenin)

© 2023 Authors. This is an open access publication, which can be used, distributed and reproduced in any medium according to the Creative Commons CC-BY 4.0 License requiring that the original work has been properly cited.

composition of the starting material. However, after the production of the can, the question of its mechanical properties under the internal pressure of the contents becomes very important.

Easy-open ends are an important part of the beverage industry, which have been made with can end stock (CES) AA5182 alloys for a long time (Hoyle & Setlak, 1996). The main function of the ends is to provide a safe closure and an easy opening (Courbon, 2000). The history of easy open ends started early. Today can-making industry utilizes the same technology as it did in the past but with some changes in the innovation aspects. In recent decades, there has been a trend to reduce end diameter and metal gauge and thus reduce costs (Yamazaki et al., 2007, 2011). In addition, reducing the amount of material used is an effective method of reducing environmental impact (Han et al., 2010). New lightweight ends have a different shape compared to the long-standing industry standard B64 end developed by Alcoa. Modified geometry of the ends would allow for the use of lighter gauge metal even if the basic diameter of the end remained unchanged. However, all these down-gauging improvements have to ensure the same properties for the ends, mainly in buckle resistance to the internal pressure within the can. Technology over the years has allowed for the manufacture of much lighter ends that must withstand the same pressure. In general, most ends are produced with a guaranteed minimum strength to resist an internal pressure of 620 kPa (90 psi) (DeWeese et al., 2008).

The pressure inside the container depends upon the drink type and temperature change. The internal pressure causes a strain on the end which induces tensile stresses in the end panel of the beverage can, which in extreme cases may lead to buckling (Yamazaki et al., 2005). Additionally, beverage can ends indicate a significant time-dependent buckle strength loss. Studies have shown that the time from the production date of the packaging also affects changes (deterioration) in the mechanical properties. In that case, the canned beverages visible on store shelves should not only be considered in terms of the expiration date for the content itself but also the packaging.

In addition to the above, during storage, transportation, and heat treatment of beverage cans, the internal pressure changes significantly. Over time and with temperature changes, the mechanical properties of the can material itself also change. This is due to both the aging processes in aluminum alloys and to the dependence of the strength of these alloys on temperature. For these reasons, the quantitative prediction of the maximum internal pressure that a can will withstand depending on factors such as time, storage

temperature, and temperature of the can material is currently an important practical problem that has not been resolved at present.

Artificial neural network-based prediction models for aluminum alloys have gained significant traction and widespread industrial application in recent years. Numerous studies have focused on developing prediction models for mechanical properties and manufacturing processes (Alibeiki et al., 2012; Lee et al., 2020; Wang et al., 2015; Zhang et al., 2019). For example, a paper by Merayo et al. (2020) introduced a computer-aided tool that predicts the plastic behavior, yield strength, and ultimate tensile strength of metallic materials. This prediction model uses the alloy's chemical composition, parameters of the tempers, and Brinell hardness as input parameters. Similarly, Sigli et al. (1996) developed a prediction model within a metallurgical simulator to estimate yield strength based on process parameters. Their model takes into account factors such as microstructure, cold rolling reduction, baking time, and temperature. By considering these variables, the model accurately predicts the yield strength. These advancements in prediction modeling using artificial neural networks have significantly contributed to the understanding and prediction of mechanical properties and the behavior of aluminum alloys during manufacturing processes.

Several reports in the literature have focused on the principles of aluminium alloy sheet processing (Hirsch, 2010) and thermal treatment temperatures (Wen & Morris, 2003; Wen et al., 2005). Yang et al. (2018) investigated the effects of the bake softening and precipitation behaviors of the AA5182-H19 sheet. Their study showed that the temperature and time of the coating processes influence the decrease in the strength and hardness of the alloys. In addition, the study was closely related to the end's area as it discussed the change in the properties of the raw material itself before its final processing before it is delivered to the can manufacturer. Picu et al. (2005) investigated the mechanical behavior of the AA5182 at temperatures ranging from -120°C to 150°C . The results showed that dynamic strain aging had an impact on ductility and strain hardening. In the work by Reid et al. (2001), the analysis of the buckling of a can with a deformed sidewall was studied. However, the buckling of an end was not investigated.

A thorough literature review shows that there is a lack of studies focused on the evaluation of material properties of the beverage end made of AA5182, especially concerning the lifetime when the product is subjected to various processes that change its quality in the context of buckling resistance.

The purpose of this work is to experimentally study the dependence of the strength of the beverage can ends on the parameters listed above and, on this basis, to develop an engineering technique for predicting the maximum allowable internal pressure in the can. Since the can ends are made to be less strong than the main material, the strength of this particular element of the can is investigated in this work. The work provides data that help in better understanding the influence of various conditions on alloy properties from the beginning to the end of the entire life cycle of the can end.

2. Materials and methods

The aluminum alloy AA5182-H48 temper, is usually used in the production process of beverage can ends. The AA5182 alloy is selected because of its favorable material properties, such as low density, high corrosion resistance, and the formability necessary for the forming of intricate shapes. The nominal chemical composition of the AA5182 base materials used in this investigation is presented in Table 1. The manufacture of AA5182 can end stock includes many steps where the coating process is carried out in the final phase. The baking times and temperature of the coating processes depend on the coating line and type of coatings. Before baking, AA5182 coils are H19 tempered, but after baking, that brings the material to the recovered stage H48. This process affects the decrease of the strength, hardness, and the increase of the elongation (Yang et al., 2018). The can end stock is received precoated with a coating. This coating on both sides of the coil serves the dual purpose of corrosion protection of the final product and as a lubricant during the stamping processes in the manufacturing process (Leggat & Taylor, 1999).

The can-making industry has two main standards; the long-standing standard B64 end and the relatively new lightweight beverage end (e.g. CDL), with the lightweight ends increasingly being used worldwide. An example of this may be seen in Figure 1, which shows a cross-section through a modern 202CDL end. The manufacturing process of the 202CDL ends is carried out by cold-forming sheets of 0.208 mm thickness (Filizzola et al., 2021).

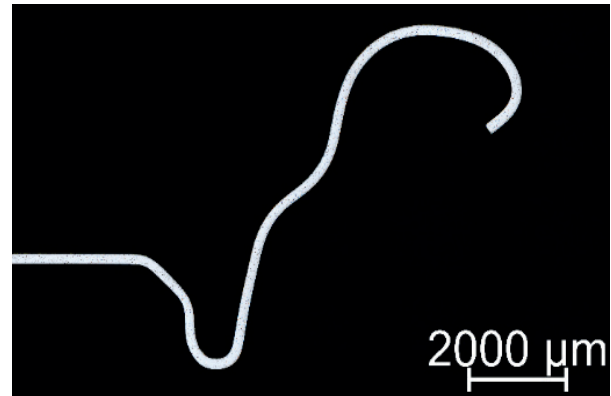


Fig. 1. Cross-section through a 202CDL can end

In this work, the ends from materials from three different suppliers (conditionally named Suppliers A, B, and C) were studied. The initial sheet material was also studied. All samples were 0.208 mm thick and made from commercial can end stock sheets. Chemical composition testing and analysis of AA5182 alloy samples were performed using the X-ray fluorescence spectrometer Shimadzu EDX-8100, and results are presented in Table 2. The results of measuring the mechanical properties of the original sheet material are shown in Table 3.

Table 1. Nominal chemical composition [wt.%] of the AA5182 alloy (Cayless, 1990)

Grade designation	Si	Fe	Cu	Mn	Mg	Cr	Zn	Ti	Unspecified other elements		Al
									each	total	
5182	0.20	0.35	0.15	0.20–0.50	4.00–5.00	0.10	0.25	0.10	0.05	0.15	remainder

Table 2. Chemical composition of the experimental samples [wt.%]

Grade designation	Si	Fe	Cu	Mn	Mg	Cr	Zn	Ti	Unspecified other elements		Al
									each	total	
Supplier A	0.048	0.175	0.053	0.352	4.432	0.086	0.022	0.011	–	0.799	94.022
Supplier B	0.039	0.200	0.080	0.368	4.294	0.080	0.012	–	–	1.144	93.783
Supplier C	0.066	0.198	0.085	0.341	4.284	0.027	0.022	–	–	0.174	94.803

Table 3. Tensile properties of the experimental samples

Tensile properties	Supplier A AA5182	Supplier B AA5182	Supplier C AA5182
YS [MPa]	346	352	353
UTS [MPa]	390	402	410
A [%]	6.7	8	7

Explanations: UTS – ultimate tensile strength; YS – yield strength; A – elongation

Buckling strength is one of the most critical parameters that must be met for beverage can ends. Figure 2 illustrates the buckling strength testing process using air pressure to test the ends. To ensure the keeping of required buckling strength for the ends, tests are carried out using dedicated equipment (see Fig. 3).

The test conditions include all the possibilities that may exist throughout the lifecycle of the ends:

- Length of storage time which is known as natural aging (aging can occur at room temperature) – the impact of long-time storage on buckle strength loss.
- Natural aging at various temperatures – the influence of warehousing temperature on the buckle strength loss of the ends.
- Accelerated aging, which is called artificial aging (aging occurs at elevated temperature) – is the influence of high temperatures after the filling process (e.g., pasteurization, sterilization) on the loss of buckle resistance. Each of the processes means heating the product, in properly designed equipment, to one of the temperatures given in the following Table 4 and holding continuously at that temperature for the corresponding specified time.

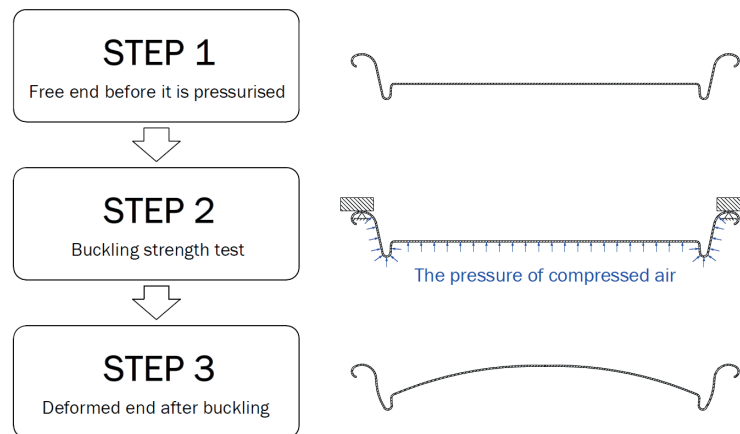
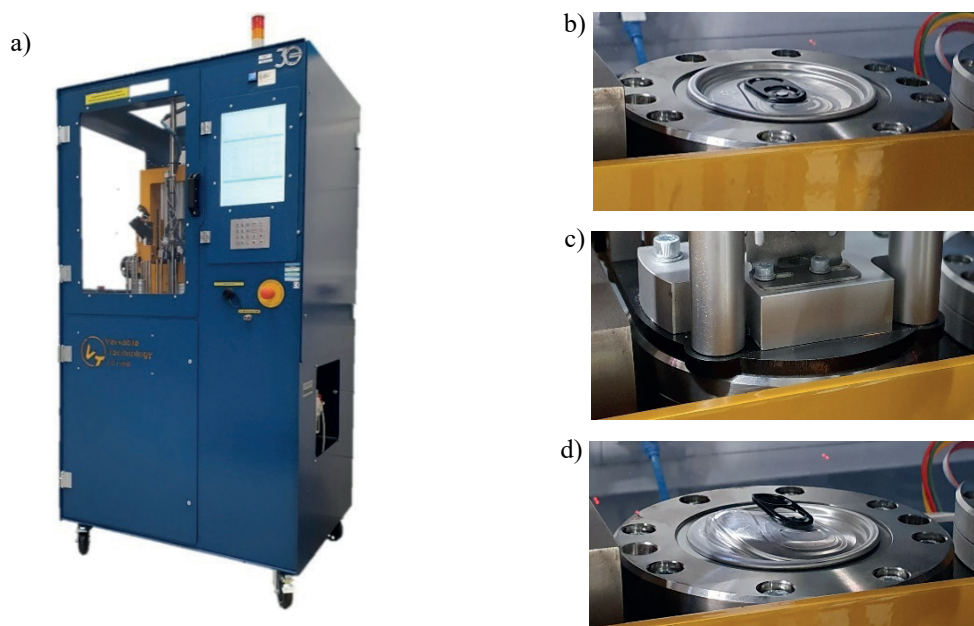
**Fig. 2.** Buckling strength testing process**Fig. 3.** Automatic buckle tester for beverage can ends: a) Machine Versatile Technology LD136B; b) the end before testing; c) buckling strength test; d) deformed end after buckling

Table 4. Conditions of typical heat treatment process beverages

Process	Type of beverage	Temperature [°C]	Time [min]
Pasteurization	beer	60–70	10–15
Pasteurization	ice tea	70–80	
Pasteurization	energy drink	80–90	
Sterilization	coffee with milk	100–121	
Sterilization UHT	milk	138–148	

The aging phenomenon also gets worse with increasing temperature. The samples were tested under various temperature conditions, thus simulating the entire life cycle of the product (ends) from their production to consumption. This means that the can is kept at different temperatures during manufacturing and storage.

The buckling strength tests were performed using an automatic beverage can end buckle gauge Versatile Technology LD136B (Fig. 3). The ends were obtained through the manufacturing process. Samples were naturally aged at 20°C and were tested on average every 7 days until the end of the entire period. The whole cycle of the natural aging process lasted 365 days. In this study, we investigated beverage can ends under buckling strength. All experiments on measuring the strength, performed on the testing device, were repeated 4 or 5 times, followed by averaging the result and estimating the standard measurement error.

Examples of beverage can end before and after the buckling test were shown in Figure 4 and Figure 5, respectively.

**Fig. 4.** Beverage can end before the buckling test**Fig. 5.** Beverage can end after the buckling test

The mechanical properties of the original sheet material at different temperatures were examined on a Zwick250 testing machine equipped with a heating device; the tensile rate was 5 mm/min. The setup and examples of samples tested at different temperatures are shown in Figure 6. The test samples were modified to be suitable for tensile tests in the temperature chambers. For this purpose, holes were made at both ends of the sample, and the use of flat fixing clamps allowed us to perform a tensile test in the environment of set temperatures. The tensile test samples were cut along the rolling direction.

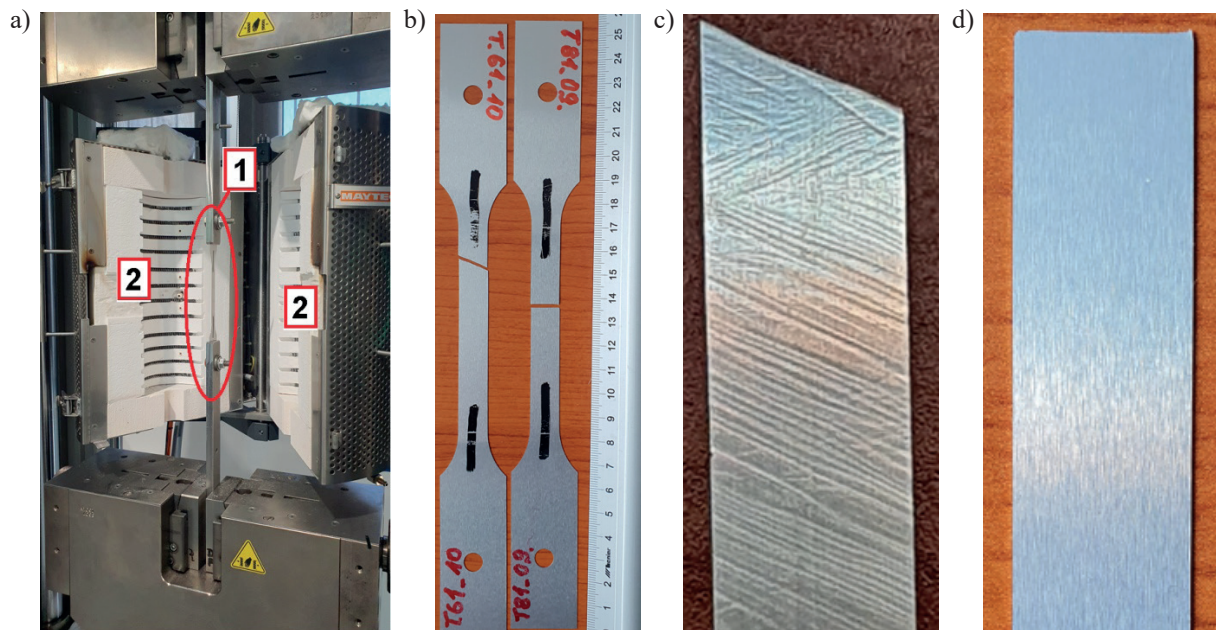


Fig. 6. Tensile test of the initial sheet material at different temperatures: a) Machine Zwick 250 for tensile tests: 1 – sample, 2 – heating device (shown open); b) selected samples after tests; c) deformed zone of the sample after tests at 61°C; d) deformed zone of the sample after tests at 81°C

Vickers hardness tests were performed using a Qness, model Q10A machine with a load of 1000 g and a loading time of 15 s. A total of five readings were taken for every aging temperature and an average value was calculated.

3. Results and discussion

3.1. Model of buckle strength loss

The mathematical model of the buckling strength of can ends is proposed in this study in the form of the following equation:

$$\sigma_{bs}(\tau, t_s, t) = \sigma_0 R_s(\tau)^{K_s(t_s)} K_t(t) \quad (1)$$

where: $\sigma_{bs}(\tau, t_s, t)$ – internal pressure leading to the destruction of the end of the can (which corresponds to its opening under the action of internal pressure) [kPa]; τ – material aging time [days]; t_s – the temperature at which the material was stored during aging [°C]; t – the temperature of the can end material at the time of the test [°C].

The parameter $R_s(\tau)$ describes the relative change in buckling strength due to natural aging at a temperature of 20°C. This parameter is defined as the ratio of the buckling strength $\sigma_{bs}(\tau)$ after time τ to the initial buckling strength σ_0 measured before the start of the aging process:

$$R_s(\tau) = \frac{\sigma_{bs}(\tau)}{\sigma_0} \quad (2)$$

The way to quantify the dependence $R_s(\tau)$ follows from its physical meaning and requires the measurement of buckling strength after various periods of aging at a temperature of 20°C. Such an experiment should be long-term to cover the possible time interval for storing the cans. In our work, its duration was 1 year with a strength measurement interval of about 1 week. In addition, in this experiment, it is necessary to average the data of several suppliers (materials from 3 suppliers were used in the paper).

The effect of aging temperature on its intensity is proposed to be taken into account by using the correction factor $K_s(t_s)$.

The expression $R_s(\tau)^{K_s(t_s)}$ is numerically equal to the ratio of the buckling strength after aging at temperature t_s $\sigma_{bs}(\tau, t_s)$ to the initial buckling strength σ_0 .

$$R_s(\tau)^{K_s(t_s)} = \frac{\sigma_{bs}(\tau, t_s)}{\sigma_0} \quad (3)$$

At a temperature of 20°C, the value of K_s should be equal to 1, then Equation (3) is transformed into Equation (2).

The proposed method for determining the relationship $K_s(t_s)$ is based on the measurement of buckling strength after aging at various temperatures. However, such an experiment is difficult to carry out over a long time interval. Therefore, we were forced to assume that it is sufficient to study the effect of short-term aging at different temperatures in order to take into account the effect of temperature. This assumption will be verified below based on an additional experiment.

In addition to the above factors associated with the effect of aging during long exposure of the can end, its buckling strength is also affected by the current temperature of the material. The influence of the current temperature on the buckling strength is proposed to be taken into account by introducing the coefficient K_t into Equation (1).

Its physical meaning is the relative change in the ultimate tensile strength (UTS) of the material at UTS with a temperature change:

$$K_t(t) = \frac{UTS}{UTS_{20}} \quad (4)$$

where UTS_{20} is the ultimate tensile strength at 20°C. At a temperature of 20°C, the value of K_t is equal to 1.

The numerical dependence of K_t can be determined based on tensile experiments on samples at different temperatures. Such an experiment requires the use of the equipment shown in Figure 6.

It is assumed in this work that the dependencies described above can be represented in the form of the following empirical equations:

$$R_s(\tau) = 1 - a \ln(\tau + 1) \quad (5)$$

$$K_s(t_s) = c_0 + c_1 t_s + c_2 t_s^2 \quad (6)$$

$$K_t(t) = \exp(b(t - 20)) \quad (7)$$

where the empirical coefficients a , b , c_0 , c_1 , and c_2 must be determined based on the experimental data.

Equations (5)–(7) were calibrated using the least squares method. The calibration procedure takes place in three stages:

1. An experimental study of the effect of long-term natural aging at a temperature of 20°C on buckling strength is carried out. The obtained experimental data are used in the equation:

$$\delta_{Rs} = \sum_{i=1}^n \left(\frac{\sigma_{bsi}(\tau)}{\sigma_0} - 1 + a \ln(\tau + 1) \right)^2 \rightarrow_{\min a} \quad (8)$$

Values $\sigma_{bsi}(\tau)$ are determined experimentally with an interval of 1–2 weeks. The number of such experiments is n , and the number of the current experiment is denoted by i . The value of σ_0 is determined once, immediately after the production process.

2. Experimental studies on the effect of artificial short-term aging at different temperatures on strength are carried out. The obtained experimental data are used to determine the coefficients of Equation (6) by minimizing the following function:

$$\delta_{Ks} = \sum_{i=1}^n \left(\frac{\sigma_{bsi}(\tau, t_s)}{\sigma_0} - c_0 - c_1 t_s - c_2 t_s^2 \right)^2 \rightarrow_{\min c_0, c_1, c_2} \quad (9)$$

The values $\sigma_{bsi}(\tau, t_s)$ are determined experimentally in experiment number i .

3. Tensile experiments are performed on the specimens shown in Figure 6. The goal is to determine the decrease in material strength (UTC) with increasing temperature. The obtained experimental data are used to determine the coefficient b :

$$\delta_{Kt} = \sum_{i=1}^n \left(\frac{UTS_i}{UTS_{20}} - \exp(b(t - 20)) \right)^2 \rightarrow_{\min b} \quad (10)$$

The values of UTS_i are determined experimentally in experiment number i .

In Equations (8)–(10), n is the number of experiments.

3.2. Experimental study of natural aging

Natural aging is a slow process, and its effects may only become significant after a few months or years. In the initial study, received ends were naturally aged for more than one year. The length of the aging period was established based on the time that typically does not exceed the storage time of filled cans in warehouses or on store shelves. The buckling strength of ends decreases rapidly during the first few days and then reaches a relatively stable condition. The major drop (20–30 kPa) takes place in the first 7–14 days after manufacturing, and it is about 50% of the total drop in 6 months. Figure 7 shows the buckling strength as a function of time at a storage temperature of 20°C for 202 CDL ends made from AA5182-H48 supplied by three different end stock producers. Long storage time, which lasted one year, has incurred a significant loss in buckle strength. The largest buckle strength loss was observed immediately after the manufacturing process. The differences for the series of sharp rises and falls, observed mainly for supplier C, depend on the geometric parameter dimensions for tested ends. Some of the geometry parameters of ends (e.g. Panel Depth) are influential for buckling strength loss. The production process based on an 8-out press delivers at the same time ends with some deviations of geometry dimensions, depending on tool condition and setup tools. At the end of this process, the final ends have random geometry parameters.

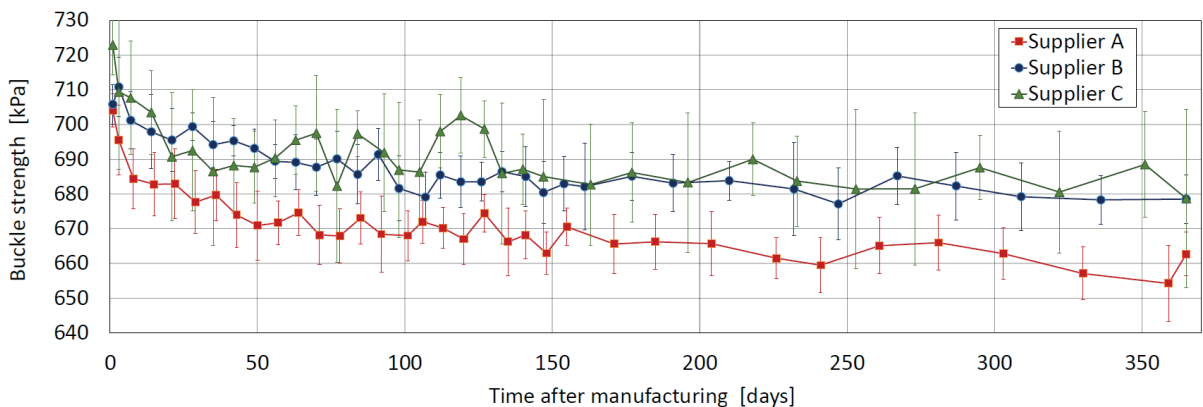


Fig. 7. Buckle strength loss at 20°C for 202 CDL ends made from AA5182-H48 supplied by three different end stock producers

The averaging of the data of three manufacturers and their reduction to a dimensionless form according to Formula (2) is shown in Figure 8. Ap-

proximation of the data obtained by Equation (5) by minimizing the error function (8) is shown in Figure 8 by the dotted line.

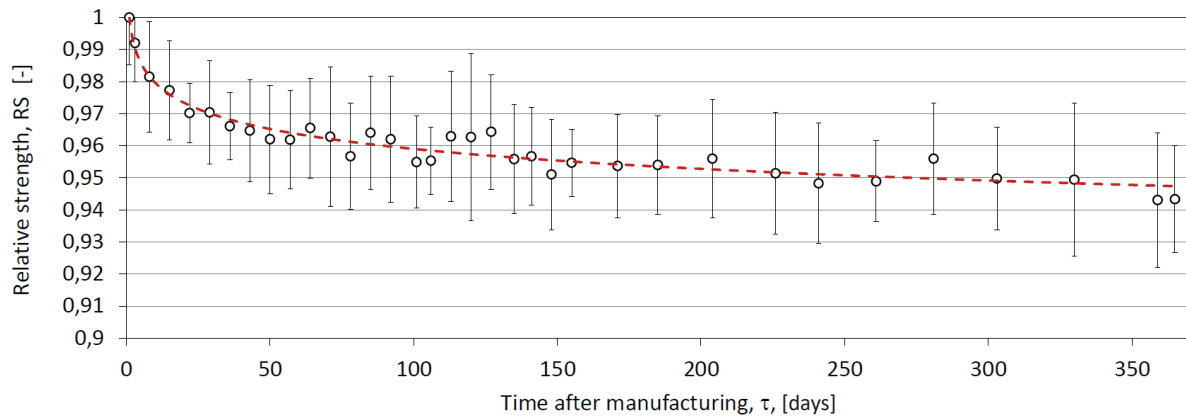


Fig. 8. Relative buckle strength (RS) at 20°C for 202 CDL ends made from AA5182-H48, averaged over three different end stock producers

3.3. Experimental study of aging at different temperatures

Studies of the influence of aging temperature on the loss of buckle strength after artificial aging were carried out for the temperature range of 20–148°C. The aging time was 15 min. In addition to measuring the buckling strength, an analysis of the end material hardness was also performed (Fig. 9). The resulting decrease in hardness with an increase in the aging temperature is natural but insignificant (1.6% when the aging temperature changes from 20°C to 148°C). The hardness test showed no significant changes be-

tween the tested sheets of aluminum alloy. In theory, the sheet (CES) should not be susceptible to aging, because after coating it was annealed by the producer of the coil. The experimentally obtained dependence of strength on the aging temperature is shown in Figure 10a. The strength of the end with the change in temperature of aging changes by about 5%. The latter proves a sensitivity to temperature aging of buckle strength greater than that of hardness.

Bringing the experimental data of buckle strength to a dimensionless form according to Formula (3) and the results of approximation based on Equations (3) and (6) are shown in Figure 10b.

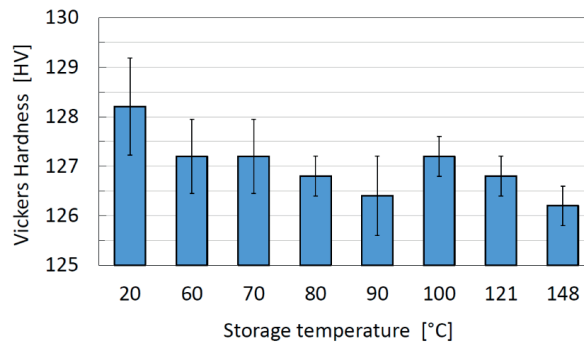


Fig. 9. Vickers hardness of 5182 alloy aged sheets

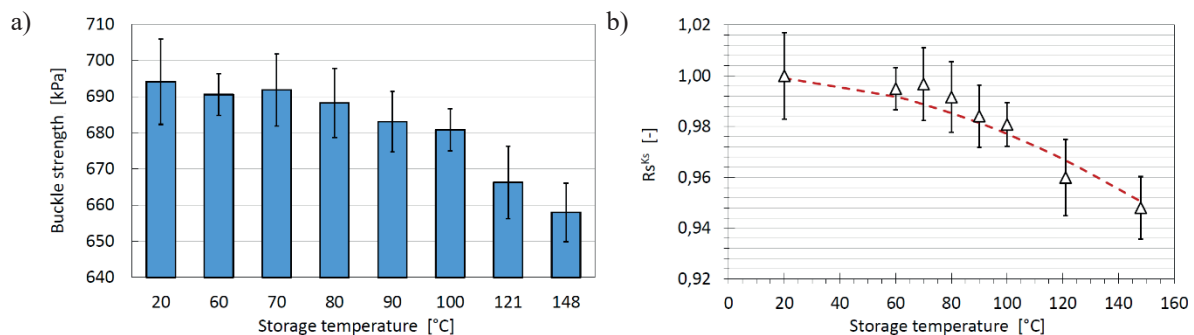


Fig. 10. Buckle strength loss after aging for 15 min at different temperatures for ends made from AA5182 (a) and corresponding relative buckle strength loss (b)

3.4. Dependence of UTS strength on the test temperature

Tensile tests were performed at temperatures between 20°C and 150°C on the setup shown in Figure 6. Examples of stress-strain curves are shown in Figure 11 as obtained at 20°C, 60°C, 100°C and 150°C. The irregular behavior in the stress-strain curves at temperatures, 20°C and 60°C, in the form of a serrated yielding phenomenon, is known as the Portevin–Le Chatelier (PLC) effect. The main factor responsible for the PLC effect is the Mg content in aluminum alloys. Serrated flow was observed in all tests performed at temperatures in the range 20°C to 80°C.

From each curve, a UTS value was obtained. These data are summarized in Figure 12a. The reduction of the experimental results to a dimensionless form was carried out according to Formula (4). Their approximation is performed using Equation (7), minimizing the squared deviations (10). The approximation results are shown in Figure 12b.

Summing up the results of the calibration of the model described by Equations (1)–(7), we present the obtained empirical coefficients:

$$a = 8.964 \times 10^{-3}; b = -0.001106; c_0 = -0.5098; \\ c_1 = -0.001148; c_2 = 0.1356.$$

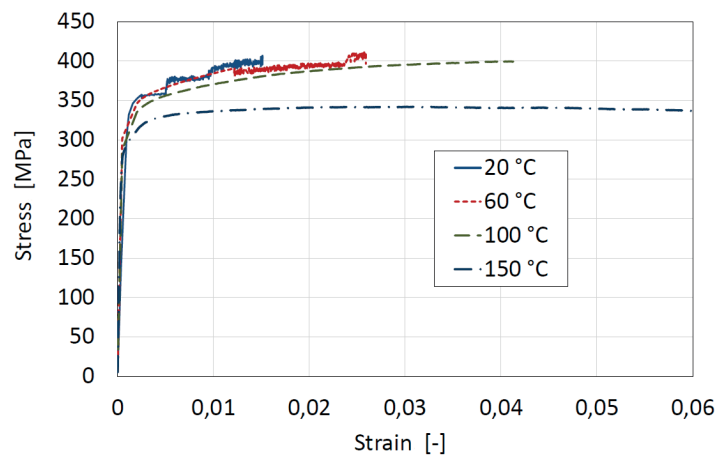


Fig. 11. Examples of stress-strain curves during tensile tests of 5182 alloy sheets at different temperatures

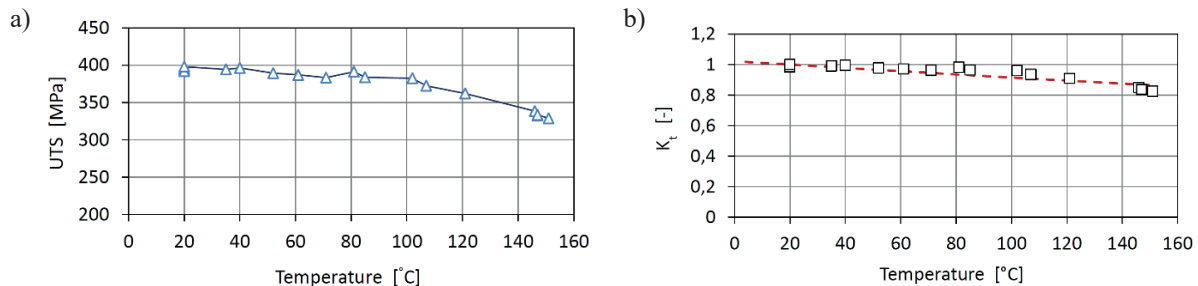


Fig. 12. Ultimate tensile strength (UTS) at different temperatures (a) and relative tensile strength K_t (b)

3.5. Model validation

To validate the developed model, an additional experiment was performed to study the effect of aging time and aging temperature on buckle strength. The following aging temperatures were used: 4°C, 20°C, and 40°C. The purpose of choosing 4°C was to test the model in an extrapolation mode. The maximum aging time was 28 days. At the end of each week, an experiment was carried out to measure the buckling strength. The results of the experiment are shown in Figure 13.

The dotted lines in this figure show the results of the buckle strength calculation according to Equation (1). Comparing the results of the calculation and the experiment, we can conclude that the accuracy of the calculation is significant and comparable to the standard error of the experiment.

Additionally, the dependence of the yield stress of the end material under the same conditions was investigated. However, the results showed (Fig. 14) that the observed change is within the measurement error, that is, it is not statistically significant.

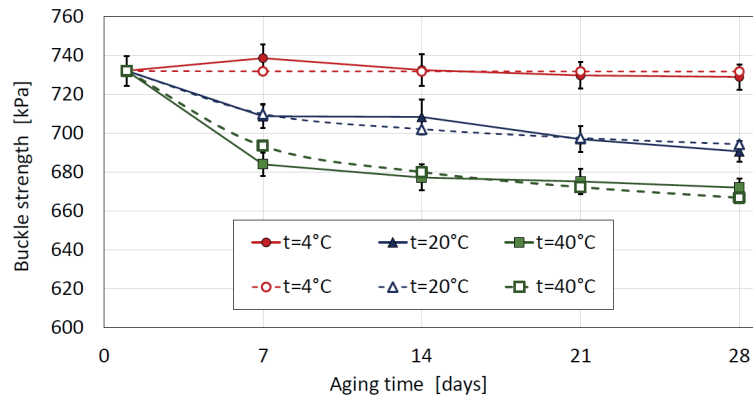


Fig. 13. The influence of warehousing temperature on can ends buckle strength loss (solid lines – experiment, dot lines – prognosis)

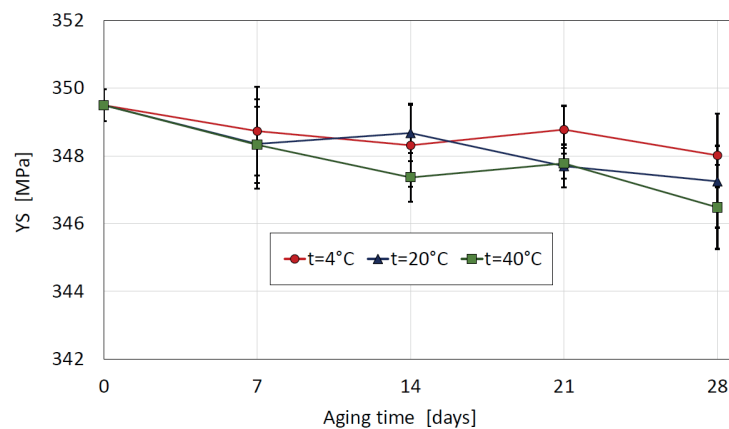


Fig. 14. The influence of warehousing temperature on YS

4. Discussion

In the process of analyzing the obtained experimental data, several important observations can be made.

A study of the dependence of hardness (Fig. 9) and yield stress (Fig. 14) on temperature and aging time showed that the observed changes in these values are not statistically significant. At the same time, the study of the buckling strength of the same material using the setup in Figure 3 yields a statistically significant result. From this, it can be concluded that the applied method of testing the influence of aging on buckle strength, based on the destruction of the ends with the help of internal pressure, is much more sensitive to changes in material properties due to aging than standard hardness and tensile tests.

A quantitative analysis of the influence of long-term aging at a temperature of 20°C showed that after a year, the decrease in the buckling strength of the end is about 5% (Fig. 8). Half of this decline occurs in the first 3–4 weeks of aging.

The strength behavior of the AA5182 alloy after cold deformation is attributed to the characteristics of its aging process. Recent studies (Filizzola et al., 2021) have shown that this alloy experiences a reduction in strength over time following the cold stamping process. This is due to the dissolution of second-phase particles, which would otherwise increase the material's strength through aging hardening. This process is accelerated with an increase in temperature. Moreover, excessive aging time may result in stress relaxation, leading to a further decrease in strength. Both the dissolution of second-phase particles and stress relaxation are diffusion processes. As is well-known, the rate of diffusion processes is high initially but decreases with time. This explains why the tested strength in Figure 8 decreases rapidly in the first days of aging (in our case, the first 7–14 days).

Comprehensive studies of the microstructural changes in the AA5182 alloy during holding at elevated temperatures were conducted in (Filizzola et al., 2021). The results confirm that the holding method used re-

duced the number of second-phase particles, which decreased the strength of the alloy.

We conducted similar microscopic experiments using an optical microscope to verify the aging mechanism in the AA5182 alloy after cold stamping under the conditions employed in our study. Figure 15 displays the microstructure of the material before aging (Fig. 15a) and after aging (Fig. 15b). These images confirm the findings reported by the authors in reference (Filizzola et al., 2021), revealing a significant decrease in the number of inclusions in the microstructure following the aging process.

In addition, considering the substantial decrease in strength observed after 7–14 days, we also examined any changes in the size of beverage can ends

during this time. For this purpose, the tests were conducted using the automatic shell inspection gauge Torus Z401. This gauge enables measurements of characteristic dimensions of beverage can ends (Fig. 16). The final value for each test was determined as the average of five samples. The inspection involved eight selectable points on each end. Table 5 presents the results of the geometric parameter dimensions of the specimens after the aging test. Errors were estimated by calculating the standard deviation based on a sample that included 40 measurement results. The obtained results indicate that the changes in dimensions were not statistically significant and the studied aging processes occur without a significant change in the shape of the can end.

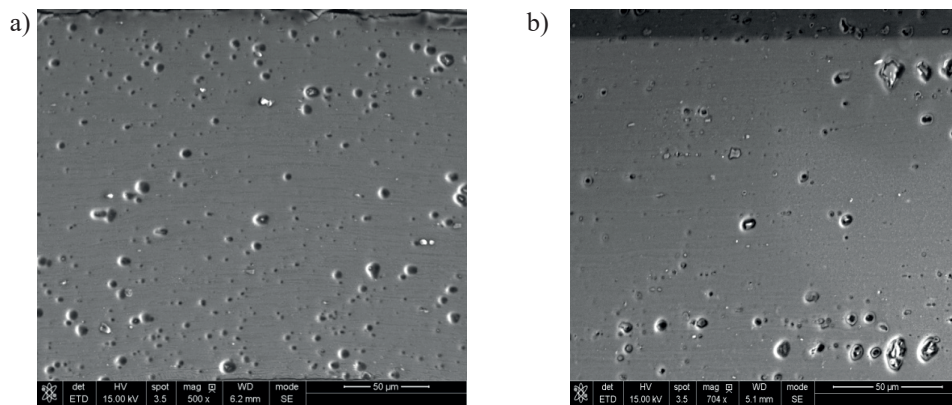


Fig. 15. Microstructure of the AA5182 alloy before (a) and after aging (b)

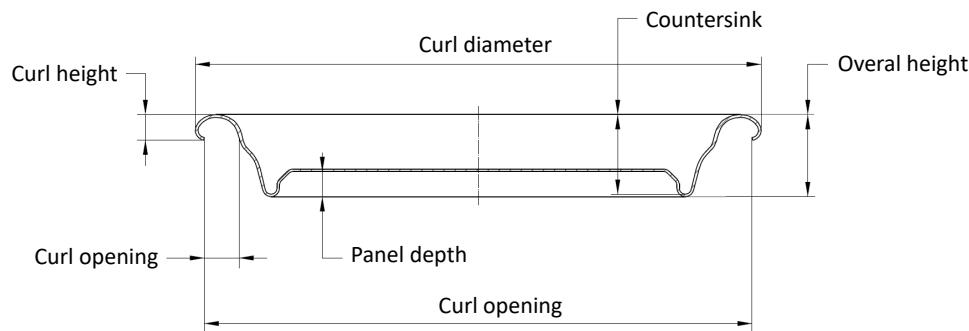


Fig. 16. Nomenclature of the geometric parameters dimensions for beverage can end

Table 5. Geometric parameters dimensions of the specimens after the aging test [mm]

Geometric parameters	0 days	7 days	14 days
Countersink	6.336 ±0.032	6.341 ±0.032	6.343 ±0.032
Panel depth	2.051 ±0.026	2.048 ±0.025	2.050 ±0.026
Curl diameter	59.285 ±0.032	59.281 ±0.031	59.282 ±0.033
Curl opening	3.054 ±0.058	3.052 ±0.058	3.059 ±0.059
Curl height	2.012 ±0.021	2.008 ±0.020	2.010 ±0.021
Inside curl diameter	57.915 ±0.056	57.909 ±0.053	57.927 ±0.060
Overall height	6.559 ±0.032	6.562 ±0.032	6.564 ±0.032

On the other hand, as the aging temperature increases, the effect of aging time on buckle strength increases sharply. Thus, the same 5% decrease in aging strength at an aging temperature of 148°C is achieved during the aging time of 15 (Fig. 10b). At 40°C per month of aging, the decrease in strength is 8% (Fig. 13). At a low temperature (4°C), no statistically significant changes in the buckling strength due to aging were recorded (Fig. 13). Thus, the experimental results confirmed that aging can significantly weaken the strength of the end of a can during storage in a hot climate. A quantitative prediction of this phenomenon is necessary for production practice.

Another interesting observation is related to the effect of temperature on the mechanism of sample deformation under tension. When the samples are stretched at temperatures below 60°C, slip bands appear on the surface of the sample (Fig. 6c). An increase in temperature above 80°C fundamentally changes the mechanism of deformation (Fig. 6d). The observed effect is also visible on the stress-strain curves (Fig. 11). The curves for low temperatures contain nonmonotonic segments. The curves for high temperatures are perfectly smooth.

Without going into the physical interpretation of this phenomenon, we note only its practical aspect in the context of the problems under consideration. The fact is that the temperature range of 60–80°C is quite achievable at different stages of processing and storing cans of drinks. This means that the noted anomalies may be of importance in the development of technology for the production and use of beverage cans. So far, we cannot draw practical conclusions from the described phenomenon, except for the quantitative dependence shown in Figure 12. However, since this effect is only observed during significant plastic deformations when the strength condition is already compromised, we believe it has minimal impact on the strength of the can end.

As for the end buckle strength engineering model developed in the article, we confirmed its performance by validation based on comparison with an independent set of experimental data. Thus, it became possible to

quantitatively predict the strength of beverage cans depending on the time and temperature of aging, as well as the temperature of the can at the time of testing. This technique can be directly used by can manufacturers to predict the maximum allowable internal pressure in a can depending on the factors listed above.

5. Conclusions

The paper is devoted to the study of the influence of aging processes on the strength of the aluminum beverage can ends. The main novelty of this study lies in simulating the complete lifespan of a beverage can ends, starting from the finishing of the production process. The tests conducted in this research elucidate the influence of different combinations of time and temperature on the alterations in the resistance to buckling of the can ends. This investigation sheds light on the mechanical behavior of beverage can ends over time and offers valuable insights into the impact of diverse environmental conditions on their structural integrity.

It is experimentally shown in the work that at 20°C, a year of aging leads to a decrease in strength by about 5%. Half of this decline occurs in the first 3–4 weeks after manufacturing. Increasing the storage temperature significantly enhances the effect of aging. For example, the storage temperature increased from 20°C to 40°C gave a two times higher drop in buckle strength in the first 7 days. In addition, a decrease in strength by 8% was observed per month of aging. This research provides insights into buckling strength loss for beverages can ends under the influence of aging. The proposed engineering mathematical model is an efficient tool to quantitatively predict the decrease in the buckling strength of the end with time, aging temperature, and test temperature, which may be suitable for use in practice. This model has proven to be a useful tool for predicting the buckling strength for beverage ends without the need for time-consuming tests, which can be the best way to cut down on complaints for can makers producing ends.

References

- Alibeiki, E., Rajabi, J., & Rajabi, J. (2012). Prediction of mechanical properties of the heat treatment by artificial neural networks. *Journal of Asian Scientific Research*, 2(11), 742–746.
- Baran, W., Regulski, K., & Milenin, A. (2022). Influence of materials parameters of the coil sheet on the formation of defects during the manufacture of deep-drawn cups. *Processes*, 10(3), 578. <https://doi.org/10.3390/pr10030578>.
- Cayless, R.B.C. (1990). Alloy and temper designation systems for aluminum and aluminum alloys. In *ASM Handbook (Vol. 2: Properties and Selection: Nonferrous Alloys and Special-Purpose Materials)*, pp. 15–28). ASM International. <https://doi.org/10.31399/asm.hb.v02.a0001058>
- Courbon, J. (2000). Mechanical metallurgy of aluminium alloys for the beverage can. *Materials Science Forum*, 331–337, 17–30. <https://doi.org/10.4028/www.scientific.net/msf.331-337.17>.

- DeWeese, S.K., Ningileri, S.T., Das, S.K., & Green, J.A.S. (2008). Stress-corrosion cracking in aluminum beverage can ends – issues, observations, and potential solutions. *JOM*, 60(5), 50–57. <https://doi.org/10.1007/s11837-008-0060-9>.
- Filizzola, D.M., da Silva Santos, T., de Miranda, A.G., da Costa, J.C.M., do Nascimento, N.R., dos Santos, M.D., Bello, R.H., del Pino, G.G., & de Macêdo Neto, J.C. (2021). Annealing effect on the microstructure and mechanical properties of AA5182 aluminum alloy. *Materials Research*, 24(4), e20200545. <https://doi.org/10.1590/1980-5373-MR-2020-0545>.
- Gong, T., Dong, J., Shi, Z., Yaer, X., & Liu, H. (2019). Effects of Ce-rich mischmetal on microstructure evolution and mechanical properties of 5182 aluminum alloy. *Materials*, 12(24), 4230. <https://doi.org/10.3390/ma12244230>.
- Han, J., Yamazaki, K., Otsuka, T., Hasegawa, T., Itoh, R., & Nishiyama, S. (2010). Thinning minimization for forming aluminum beverage can end shells. *13th AIAA/ISSMO Multidisciplinary Analysis and Optimization Conference, 13–15 September 2010, Forth Worth, Texas*, 1–10. <https://doi.org/10.2514/6.2010-9045>.
- Hirsch, J. (2010). 23 – Aluminium sheet fabrication and processing. In R. Lumley (Ed.), *Fundamentals of Aluminium Metallurgy: Production, Processing and Applications* (pp. 719–746). Woodhead Publishing. <https://doi.org/10.1533/9780857090256.3.719>.
- Hosford, W.F., & Duncan, J.L. (1994). The aluminum beverage can. *Scientific American*, 271(3), 48–53. <https://doi.org/10.1038/scientificamerican0994-48>.
- Hoyle, W.C., & Setlak, F.R. (1996). Trends and needs in can stock: A packaging company's perspective. *JOM*, 48(11), 33–36. <https://doi.org/10.1007/BF03223241>.
- Kaufman, J.G. (2000). *Introduction to Aluminium Alloys and Tempers*. ASM International.
- Lee, K., Hong, Ch., Lee, E.-H., & Yang, W.H. (2020). Comparison of artificial intelligence methods for prediction of mechanical properties. *IOP Conference Series: Materials Science and Engineering*, 967(1), 012031. <https://doi.org/10.1088/1757-899X/967/1/012031>.
- Leggat, R.B., Taylor, S.R. (1999). Effect of micron-scale surface deformation on the corrosion behavior of coil-coated aluminum alloy 5182. *Corrosion*, 55(10), 984–990. <https://doi.org/10.5006/1.3283935>.
- McMahon, M.E., Steiner, P.J., Lass, A.B., & Burns, J.T. (2017). The effect of loading orientation on the stress corrosion cracking of Al-Mg alloys. *Corrosion*, 73(6), 713–723. <https://doi.org/10.5006/2343>.
- Merayo, D., Rodríguez-Prieto, A., & Camacho, A.M. (2020). Prediction of mechanical properties by artificial neural networks to characterize the plastic behavior of aluminum alloys. *Materials*, 13(22), 5227. <https://doi.org/10.3390/ma13225227>.
- Picu, R.C., Vincze, G., Ozturk, F., Gracio, J.J., Barlat, F., & Maniatty, A.M. (2005). Strain rate sensitivity of the commercial aluminum alloy AA5182-O. *Materials Science and Engineering: A*, 390(1–2), 334–343. <https://doi.org/10.1016/j.msea.2004.08.029>.
- Reid, J.D., Bielenberg, R.W., & Coon, B.A. (2001). Indenting, buckling and piercing of aluminum beverage cans. *Finite Elements in Analysis and Design*, 37(2), 131–144. [https://doi.org/10.1016/S0168-874X\(00\)00027-5](https://doi.org/10.1016/S0168-874X(00)00027-5).
- Sigli, C., Vichery, H., & Grange, B. (1996). Computer assisted metallurgy for non heat treatable aluminum alloys. *Materials Science Forum*, 217–222, 391–396. <https://doi.org/10.4028/www.scientific.net/msf.217-222.391>.
- Wang, Y., Krane, M.J.M., & Trumble, K.P. (2015). Thermal stress prediction in AA5182 rectangular ingots. In M. Hyland (Ed.), *Light Metals 2015* (pp. 865–870). Wiley. <https://doi.org/10.1002/9781119093435.ch145>.
- Wędrychowicz, P., Kustra, P., Paćko, M., & Milenin, A. (2021). A flow stress model of the AA3104-H19 alloy for the FEM simulation of the beverage can manufacturing process under large plastic deformations. *Materials*, 14(21), 6408. <https://doi.org/10.3390/ma14216408>.
- Wen, W., & Morris, J.G. (2003). An investigation of serrated yielding in 5000 series aluminum alloys. *Materials Science and Engineering: A*, 354(1–2), 279–285. [https://doi.org/10.1016/S0921-5093\(03\)00017-0](https://doi.org/10.1016/S0921-5093(03)00017-0).
- Wen, W., Zhao, Y., & Morris, J.G. (2005). The effect of Mg precipitation on the mechanical properties of 5xxx aluminum alloys. *Materials Science and Engineering: A*, 392(1–2), 136–144. <https://doi.org/10.1016/j.msea.2004.09.059>.
- Yamazaki, K., Itoh, R., Han, J., Watanabe, M., & Nishiyama, S. (2005). Optimum design of aluminum beverage can ends using structural optimization techniques. *AIP Conference Proceedings*, 778 A(2005), 719–724. <https://doi.org/10.1063/1.2011307>.
- Yamazaki, K., Itoh, R., Watanabe, M., Han, J., & Nishiyama, S. (2007). Applications of structural optimization techniques in light weighting of aluminum beverage can ends. *Journal of Food Engineering*, 81(2), 341–346. <https://doi.org/10.1016/j.jfoodeng.2006.10.031>.
- Yamazaki, K., Otsuka, T., Han, J., Hasegawa, T., & Shirasawa, T. (2011). New tooling system for forming aluminum beverage can end shell. *AIP Conference Proceedings*, 1383, 879–886. <https://doi.org/10.1063/1.3623698>.
- Yang, Y., Zhao, P.Z., Zou, L.Y., & Fan, R.H. (2018). Bake precipitation behavior in AA5182 sheet for can end stock. *Materials Science Forum*, 913, 37–42. <https://doi.org/10.4028/www.scientific.net/MSF.913.37>.
- Yang, Y., Zhao, P.Z., Xiao, X., & Zheng, X.B. (2020). Effect of Cu content on ageing behavior for aa3104-h19 can body sheet. *Materials Science Forum*, 993, 358–364. <https://doi.org/10.4028/www.scientific.net/MSF.993.358>.
- Zhang, Q., Luan, X., Dhawan, S., Politis, D.J., Du, Q., Fu, M.W., Wang, K., Gharbi, M.M., & Wang, L. (2019). Development of the post-form strength prediction model for a highstrength 6xxx aluminium alloy with pre-existing precipitates and residual dislocations. *International Journal of Plasticity*, 119, 230–248. <https://doi.org/10.1016/j.ijplas.2019.03.013>.
- Zhu, Z., & Starink, M.J. (2008). Age hardening and softening in cold-rolled Al-Mg-Mn alloys with up to 0.4 wt% Cu. *Materials Science and Engineering: A*, 489(1–2), 138–149. <https://doi.org/10.1016/j.msea.2007.12.019>.

